

Dynamics of Charge Carriers in Silicon Nanowire Photoconductors Revealed by Photo Hall Effect Measurements

(Supporting Information)

Kaixiang Chen¹, Xiaolong Zhao², Abdelmadjid Mesli³, Yongning He^{2*} and Yaping Dan^{1,2*}

¹ State Key Laboratory of Advanced Optical Communication Systems and Networks, University of Michigan-Shanghai Jiao Tong University Joint Institute, Shanghai Jiao Tong University, 800 Dong Chuan Road, Shanghai 200240, China

² School of Microelectronics, Xi'an Jiao Tong University, 28 Xian Ning Road, Xi'an, Shaanxi Province 710049, China

³ Institut Matériaux Microélectronique Nanosciences de Provence, UMR 6242 CNRS, Université Aix-Marseille, 13397 Marseille Cedex 20, France

*To whom correspondence should be addressed:

yaping.dan@sjtu.edu.cn

yongning@mail.xjtu.edu.cn

1. Gain and Photoresponsivity Calculation Equations

Definition of gain G expressed in quantum efficiency and photo responsivity R_{PH} ¹:

$$G = \frac{J_L/e}{\frac{I_{Li}}{hc} \lambda}, \quad (S1)$$

and

$$R_{PH} = \frac{eG}{hc} \lambda, \quad (S2)$$

Where J_L , I_{Li} are the photocurrent density and illumination intensity, respectively. h , c and λ are Planck constant, light velocity and wavelength, respectively.

2. Derivation of Hall Effect Equations

As known, Hall resistance is a function of magnetic field intensity B and charge carrier concentrations, which is governed by the following equation².

$$R_H = \frac{B}{et} \frac{p\mu_p^2 - n\mu_n^2}{(p\mu_p + n\mu_n)^2} \quad (S3)$$

in which e is the unit charge, t the nanowire thickness, μ_n and μ_p the electron and hole mobility, and n and p the electron and hole concentration, respectively. We assume that the Hall and electric-field mobility are the same.

The four-probe measurements will provide the nanowire resistance which is related to the carrier concentration and mobility as shown in *eq.S4*.

$$R = \frac{L}{eWt(p\mu_p + n\mu_n)} \quad (S4)$$

in which L and W are the nanowire physical length and width, respectively. The rest of the symbols have the same physical meaning as in *eq.S3*. Similarly, for a highly doped p-type silicon nanowire, the resistance can be simplified as $R = L/(eWt\mu_p)$.

Under light illumination, the electron and hole concentration can be written as $n = n_0 + \Delta n$ and $p = p_0 + \Delta p$, where n_0 and p_0 are the electron and hole concentration in the dark, and Δn and Δp are the excess electron and hole concentration, respectively. To find the excess charge carrier concentration, let us first replace the term $p\mu_p + n\mu_n$ in the denominator on the right of *eq.S3* with an experimentally measured parameter R in *eq.S4*. After properly reformulated, *eq.S3* can be rewritten as

$$R_H = eR^2B(p\mu_p^2 - n\mu_n^2)tW^2/L^2 \quad (S5)$$

We can find the concentration of photogenerated excess charge carriers as *eq.S6* by finding $p_0\mu_p^2 - n_0\mu_n^2$ and $(p_0 + \Delta p)\mu_p^2 - (n_0 + \Delta n)\mu_n^2$ from *eq.S5*.

$$\Delta p - \frac{\mu_n^2}{\mu_p^2}\Delta n = \frac{L^2}{e\mu_p^2W^2t} \cdot \left(\frac{dR_H}{dB} - \frac{dR_{H0}}{R_0^2} \right) \quad (S6)$$

where R_0 , R_{H0} , R and R_H are the nanowire resistance and Hall resistance in the dark and under light illumination, respectively.

We can also find the concentration of excess charge carriers from *eq.S4*, which is expressed as

$$\Delta p + \frac{\mu_n}{\mu_p}\Delta n = \frac{L}{e\mu_pWt} \cdot \left(\frac{1}{R} - \frac{1}{R_0} \right) \quad (S7)$$

where R_0 and R are the nanowire resistance in the dark and under light illumination, respectively.

The hole mobility can be derived on the condition of $p_0 \gg n_0$ as the following equation *eq.S8*.

$$\mu_p = \frac{L}{W_0} \frac{dR_{H0}}{R_0 dB} \quad (S8)$$

The effective channel width W can be found by reformulating *eq.S3* and *eq.S4* on the assumption of $\Delta n + n_0 \ll \Delta p + p_0$.

$$W \approx \frac{L}{\mu_p} \frac{dR_H}{R dB} \quad (S9)$$

3. Experimental Results of Bulk Silicon Photoconductor

To compare with the experimental results for SiNWs, we performed some new experiments for bulk silicon photoconductors. Since the surface to volume ratio for bulk photo conductors is relatively low, the surface states and surface depletion region will not localize a large number of excess minority charge carriers. As a result, the concentration of excess holes and electrons in the device are nearly the same. Fig. S1 shows the bulk silicon device on a PCB platform. The thickness, width and length of the bulk silicon are 30 μm , 4.953mm and 5.842mm respectively.

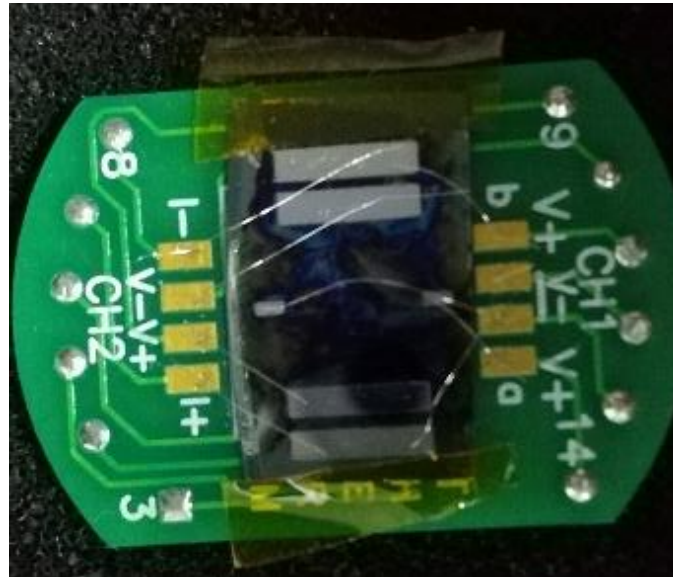


Fig. S1 Optical image for the bulk silicon photoconductor and electric circuits for test in the PPMS.

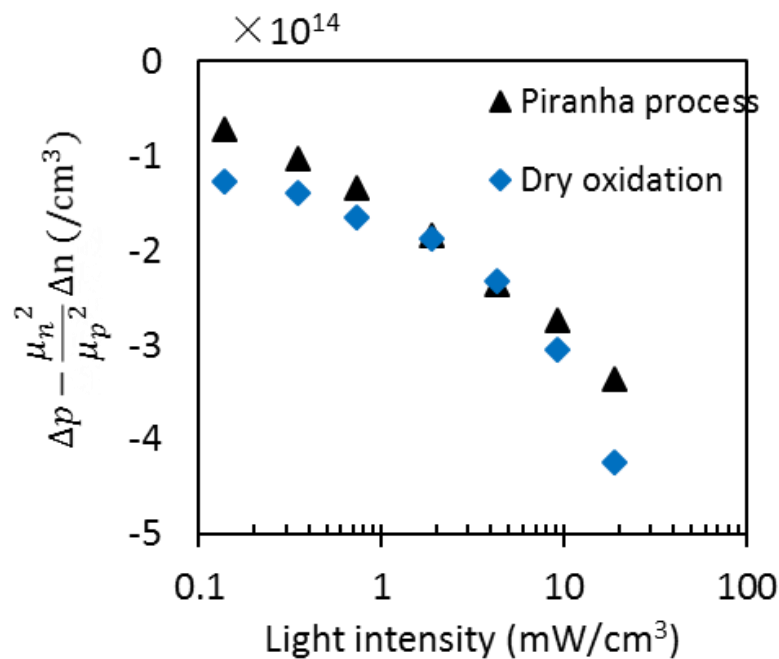


Fig. S2. $\Delta p - \frac{\mu_n^2}{\mu_p^2} \Delta n$ for a p-type bulk silicon photoconductor ($2 \times 10^{15}/\text{cm}^3$) passivated by piranha solution and dry oxidation used as a reference

for silicon nanowire photoconductors.

4. Optoelectronic Characteristics for SiNWs Doped at $1.07 \times 10^{17} \text{ cm}^{-3}$

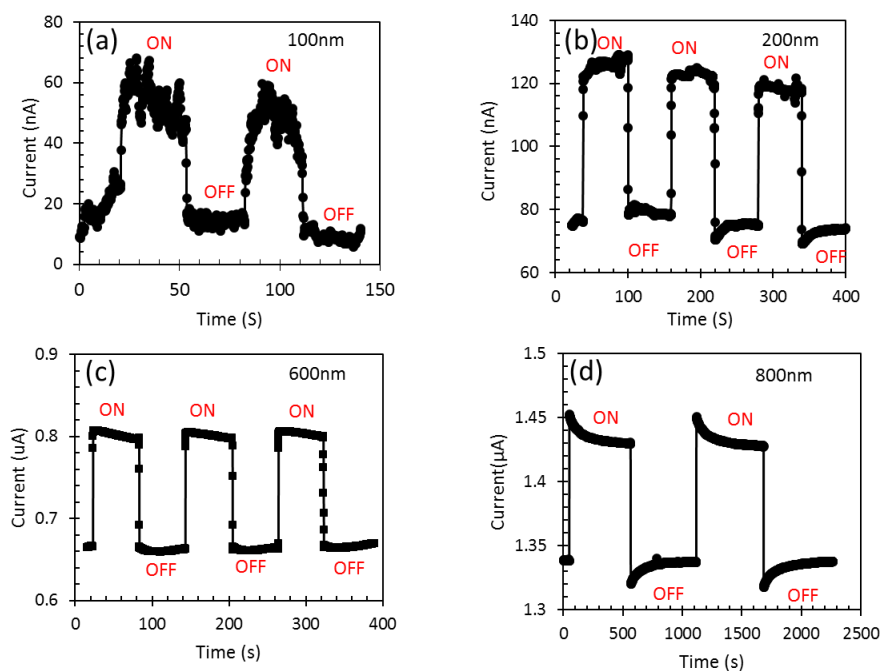


Fig. S3 Transient Current response of SiNWs with different width (nominal width 100nm to 800nm) as light illumination is periodically switched on/off (accordingly high/low in current). The external voltage is 1V and the illumination intensity is 19 mW/cm².

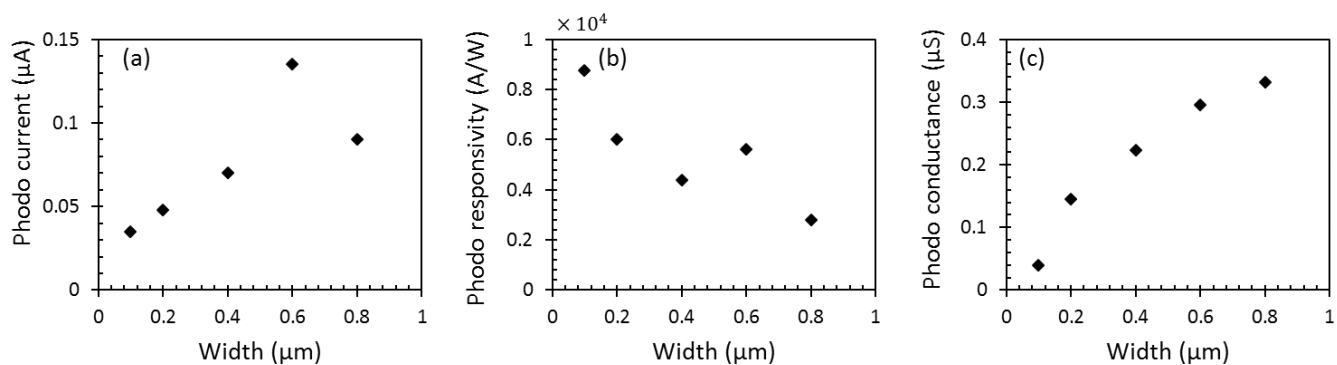


Fig. S4 Photoresponse of SiNWs with different width (nominal width 100nm to 800nm) under illumination for (a) photocurrent (measured by 2 - probe), (b) photoresponsivity and (c) photoconductance (measured by 4 - probe). The bias voltage is 1V and the illumination intensity is 19mW/cm².

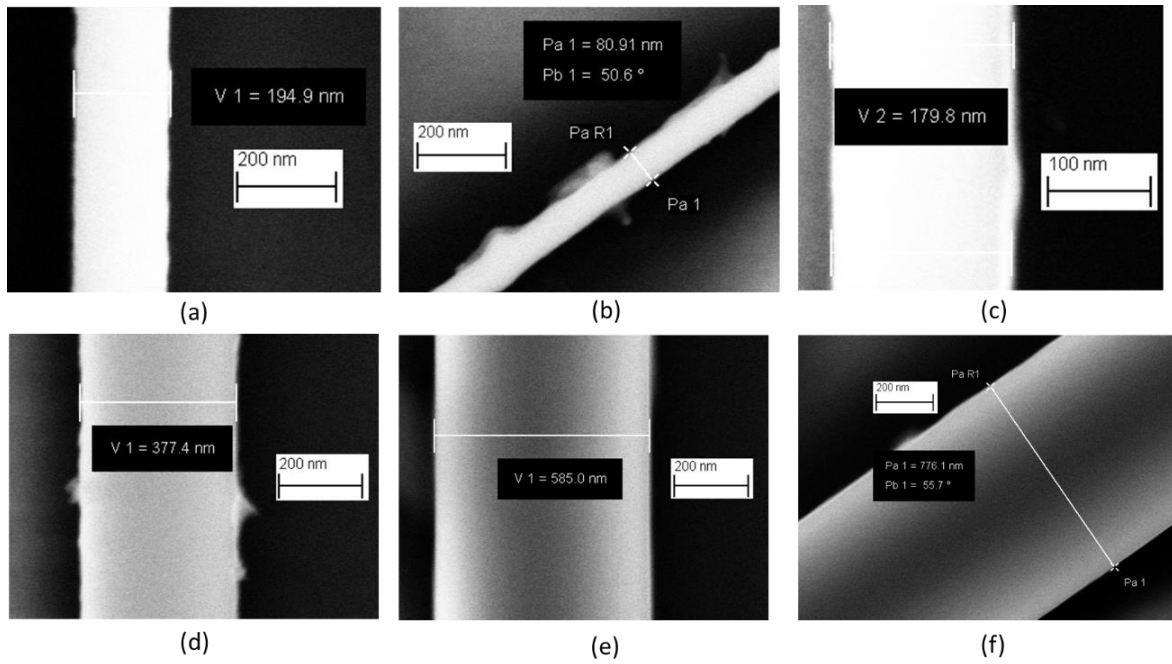


Figure S5. SEM images to show the actual width of the silicon nanowires after the surface SiO₂ is removed by HF.

Table 1. Nominal width and actual physical width for silicon nanowires under test.

Nominal width	Actual physical width
100 nm	81 nm
200 nm	188 nm
400 nm	377 nm
600 nm	585 nm
800 nm	776 nm

5. Photo Hall Effects for SiNWs with High Doping Concentration

We repeated the fabrication of p-type SiNWs with high doping concentration. The dopant concentration measured by Hall effect is $1.7 \times 10^{18}/\text{cm}^3$.

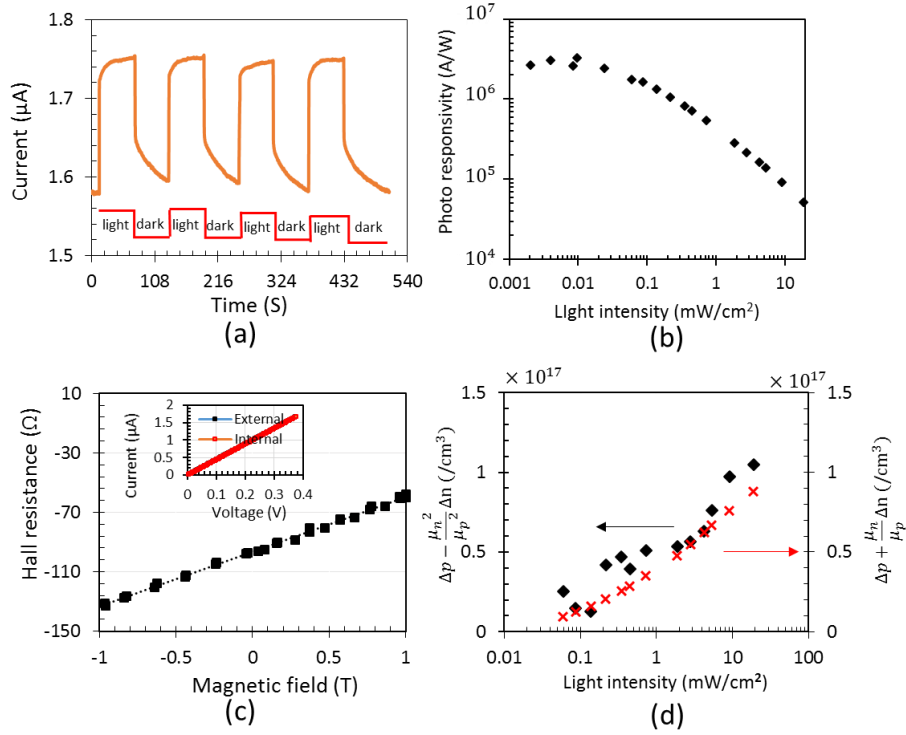


Figure S6. Optoelectronic properties for the 200nm wide SiNW at high doping level without passivation process. (a) Transient photo response as light illumination is periodically switched on/off. (b) Photoresponsivity plotted *versus* light illumination intensity. The device is biased at 1V. (c) Hall resistance as a function of magnetic field intensity. Inset: Current-Voltage (I-V) characteristics of 2-probe (Internal) and 4-probe (External) measurements. (d) $\Delta p - \frac{\mu_n^2}{\mu_p^2} \Delta n$ and $\Delta p + \frac{\mu_n}{\mu_p} \Delta n$ at different light intensity.

6. Excess charge carrier concentration after the photo modulation of the channel width is taken into account

The channel width will be modulated by light illumination. Clearly, W and t are not constant under light illumination. *eq.S6* and *eq.S7* must be rewritten as *eq.S6'* and *eq.S7'*, respectively, in which the “0” subscript denotes the parameter in the dark.

$$\Delta p - \frac{\mu_n^2}{\mu_p^2} \Delta n = \frac{L^2}{e\mu_p^2 W^2 t} \cdot \frac{dR_H}{dB} - \frac{L^2}{e\mu_p^2 W_0^2 t_0} \frac{dR_{H0}}{dB} \quad (\text{S6}')$$

$$\Delta p + \frac{\mu_n}{\mu_p} \Delta n = \frac{L}{e\mu_p W t} \cdot \frac{1}{R} - \frac{L}{e\mu_p W_0 t_0} \cdot \frac{1}{R_0} \quad (\text{S7}')$$

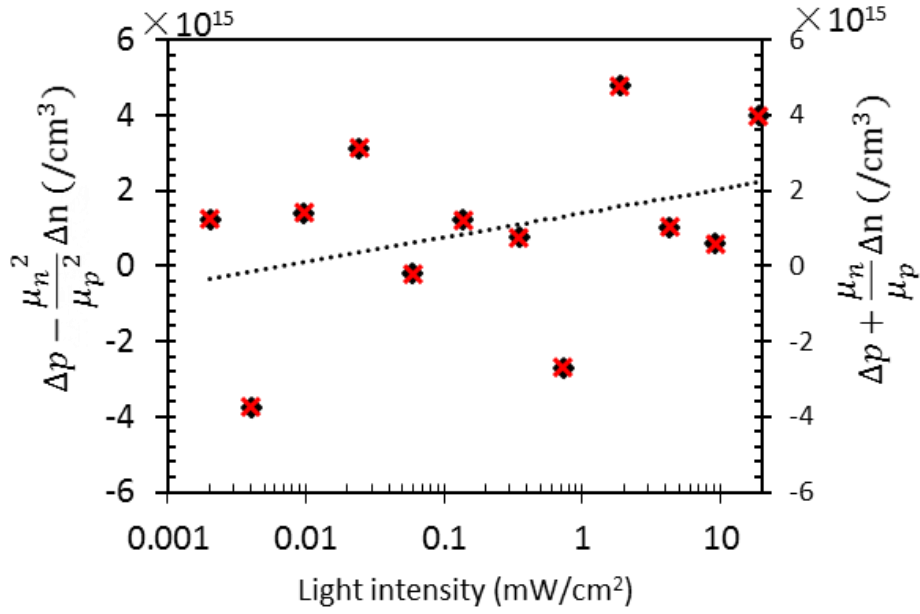


Figure S7 $\Delta p - \frac{\mu_n^2}{\mu_p^2} \Delta n$ and $\Delta p + \frac{\mu_n}{\mu_p} \Delta n$ averaged over the effective width for the SiNW ($\sim 10^{17} \text{ cm}^{-3}$, 377nm width) after taking into account the variation of depletion region width.

$\Delta p - \frac{\mu_n^2}{\mu_p^2} \Delta n$ and $\Delta p + \frac{\mu_n}{\mu_p} \Delta n$ becomes much lower when the expansion of the channel width is taken into account. It indicates the most of photo carriers move to fill in the depletion layer, resulting in the photo modulation of the depletion region width.

7. Simulation results for SiNWs with fixed charges and/or surface states

The two dimensional simulations with surface states were performed using Silvaco Atlas software. We assumed that the nanowire length and width are $9\mu\text{m}$ and 380nm , respectively. The nanowire surfaces are covered with a layer of silicon oxide, as shown in Fig. S8. The density of surface states at the SiNW surfaces is shown in the inset of Fig.4c.

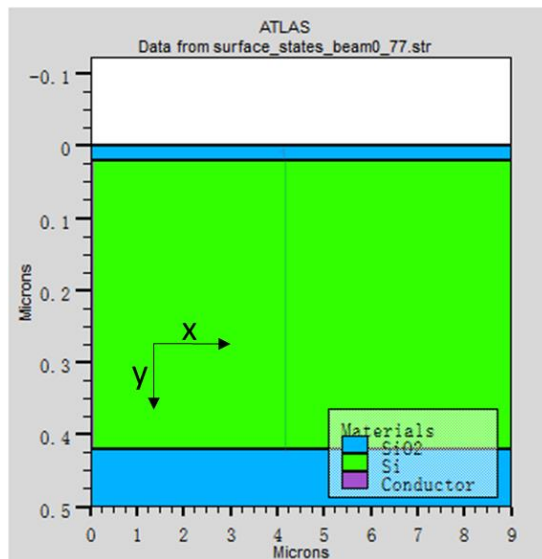


Figure S8. Cross-section along the nanowire axial direction. Left and right ends are electrodes.

We consider the following two cases in our simulations.

In the first case, there are only positive fixed charges with no surface states on the surface. The fixed charge cannot act as trapping states or recombination centers. By assuming the positive fixed charge density as $Q_F = 8.9 \times 10^{11}/cm^2$, the potential barrier at surface resulting from simulations is $\sim 0.6eV$. The depletion layer width X can be further calculated by

$$X = \sqrt{\frac{2\varepsilon_r\varepsilon_0\Delta V}{qN_A}}, \quad (S10)$$

where ΔV is the surface energy band bending, and ε and q are the Si dielectric constant and unit electron charge, respectively. The X is calculated as 85.7nm.

The depletion region can be also inferred from the nanowire channel conductance. It is known that the dark current can be expressed as

$$I \cong pq\mu_p tWE \quad (S11),$$

where W is the effective conduction channel width of the nanowire. By adding fixed charges, the channel width will be smaller than the physical width (377nm). In the simulations, the conductance of the nanowire with no surface charges is $16.7\mu S$. With the surface charges, the nanowire conductance becomes $9.1\mu S$, from which the depletion layer width X can be inferred to be 86.4 nm.

In short, the depletion layer width can be calculated from the potential barrier or dark current. Both are $\sim 86nm$, close to the experimental results.

In the second case, we assume that both fixed charge ($Q_F = 9 \times 10^{11}/cm^2$) and surface states exist on the nanowire surfaces. A potential barrier of $0.6eV$ and a depletion layer thickness of $\sim 86nm$ in the dark can be obtained by using the surface state profile shown in the inset of Fig.4c.

The depletion layer width variation with light intensity (Fig. 3d in the manuscript) in nanowire can be calculated from eq. S9.

Nanowires with a high density of surface states normally have a slow photo response speed. In the simulation, we found that the smaller capture cross section will lead to smaller 3dB bandwidth of photo frequency response (Fig. S9). The capture cross section of surface states for silicon nanowire with SiO_2 layer is seldom reported. For bulk silicon with surface passivation layer of SiO_2 , the effective capture cross section has been reported³ as $\sim 2 \times 10^{-20}cm^2$. Fig. S9 shows the photo responsivity in the excitation frequency domain with a capture cross section of $8 \times 10^{-20}cm^2$ (blue line) and $8 \times 10^{-21}cm^2$ (red line). If there are only fixed charges, the nanowire should have a bandwidth over 100KHz (Fig.S10), which is inconsistent with the experiment results. The simulations indicate that the low bandwidth likely originates from the slow trapping process by surface states.

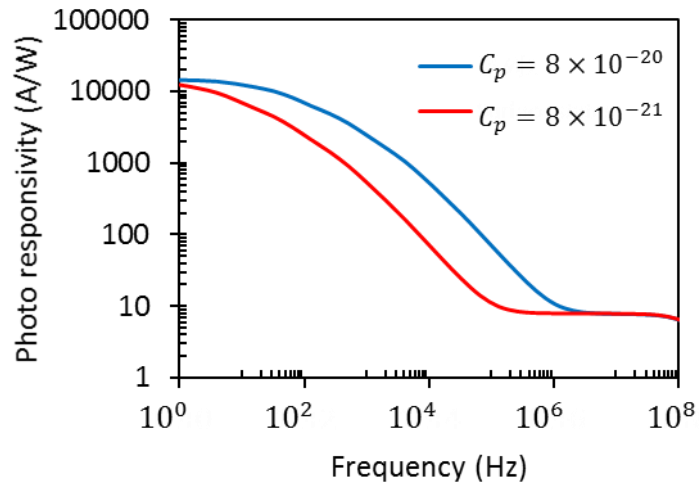


Figure S9. Frequency dependent photoresponsivity for the nanowire with surface capture cross sections $\sigma_p = 8 \times 10^{-20} \text{ cm}^2$ (blue line) and $8 \times 10^{-21} \text{ cm}^2$ (red line). The light intensity in the simulation is 19 mW/cm^2 .

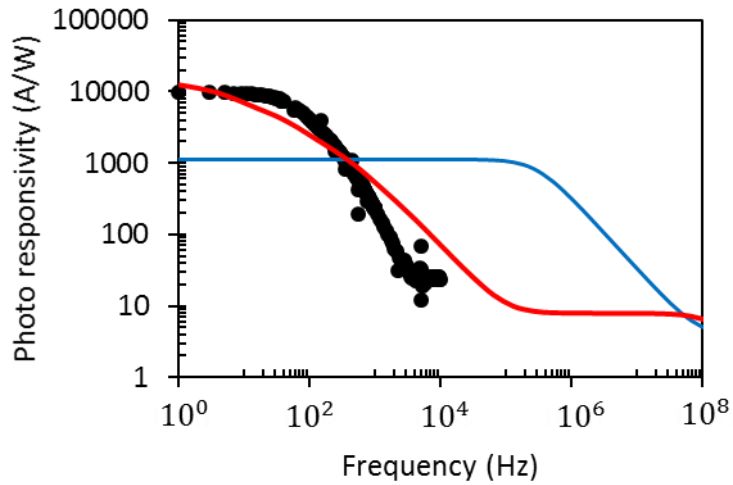


Figure S10. Simulation results of photo responsivity versus optical frequency with fixed charge only ($8.9 \times 10^{11} \text{ cm}^{-2}$, blue solid line) and with both surface states and fixed charges (red solid line). The experimental data for SiNW with 377 nm (low doping level) are plotted in black dots. The modulated light illumination intensity is 19 mW/cm^2 .

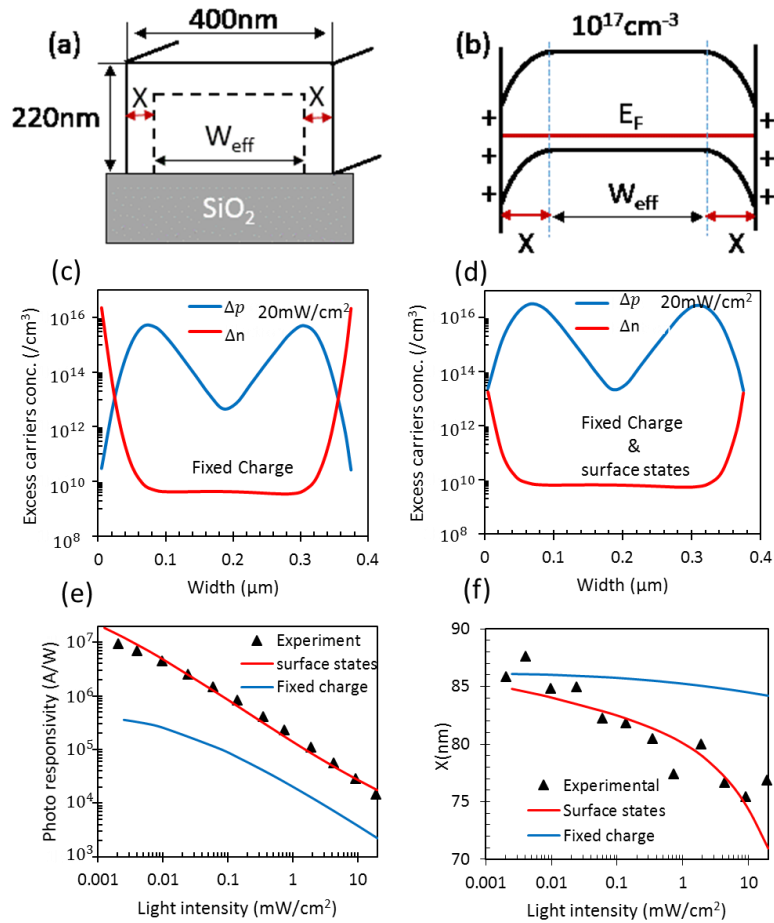


Figure S11. (a) Nanowire cross-sectional schematic where X is the depletion layer width and W_{eff} the effective channel width. (b) Energy band diagram with a net fixed surface charge of $8.9 \times 10^{11}/\text{cm}^2$. (c) Radial profile of excess electrons and holes inside the nanowire with only fixed charge (no surface states). (d) Radial profile of excess electrons and holes inside the nanowire with surface states and fixed charges. (e) Photoresponsivity as a function of light illumination intensity. (f) Depletion region width at different light illumination intensity. For both Panel e and f, red line is for the case that surface states and fixed charges coexist while blue line is for the case that only fixed charges exist.

8. Photo spectral response for SiNWs

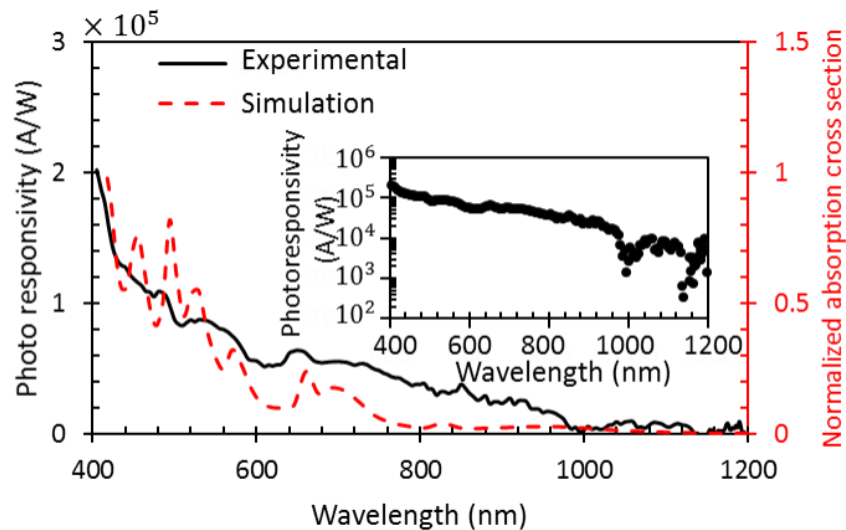


Figure S12. Spectral response for SiNW 200 nm thick at a doping concentration of $\sim 10^{18}/\text{cm}^3$. Normalized absorption cross section are simulated by Lumerical FDTD software.

We also measured and simulated the spectral responsivity of SiNW. Photocurrent and absorption peaks due to leaky mode resonances are observed. In experiment, to avoid the effect of the slow surface states, about 10 s is maintained between two wavelength points as the wavelength is swept from 1200 nm to 400 nm. In the FDTD simulation, the SiNW is designed to have a thickness of 210 nm on top of an infinitely thick SiO₂ substrate. At wavelengths that are longer than the Si absorption edge (~1100nm), the photoconductor shows a photoresponsivity as high as $10^3 - 10^4$ A/W, significantly higher bulk Si photoconductors⁴ and Si nanowire bipolar phototransistors⁵ at similar spectral range. In the bulk Si photoconductor, the photogain of the device is small while in Si nanowire bipolar phototransistor where the device photogain is high, the absorption coefficient beyond the Si absorption edge is very small.

9. LED Characteristics

We used a commercial LED (LILUN, 10W) as the illumination light source and the emission central wavelength is 460 nm with a full width at half maximum (FWHM) of ~20 nm. The LED emission intensity is monitored with a commercial high speed silicon PIN photodetector (LSSPD-0.5, 3dB bandwidth ~ 1GHz). The photodetector has a responsivity of ~2mA/mW at 460nm. The largest and minimal responsivity of the photodetector is ~6mA/mW at 400nm and ~1mA/mW at 1100 nm. By our estimation, the error of the light illumination intensity of the LED in the full spectral range will not be greater than 2 - 3 times.

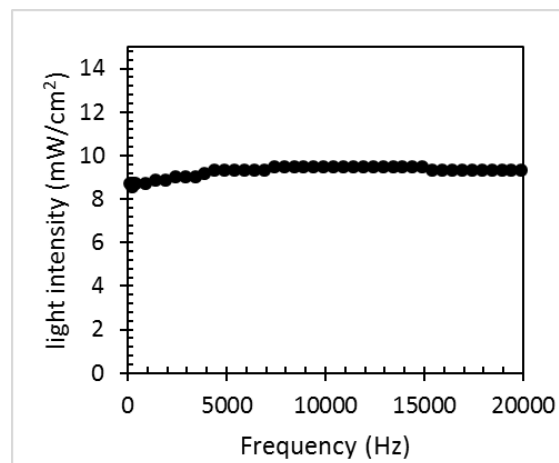


Figure S13. Frequency dependent Light intensity of the LED under a specific bias.

In our work, the nanowire photoresponsivity *versus* light modulation frequency was measured. Instead of using a mechanical chopper to modulate the light ON/OFF (difficult to do so in the PPMS system), we electrically modulated the emission of the LED. The light intensity of the LED may decay at high frequencies. To test the bandwidth of the LED, we used the commercial PIN photodetector with a bandwidth of ~1GHz to monitor the light intensity of LED *vs* the twinkle frequency. A lock-in amplifier was applied to extract the photocurrent amplitude. From Fig. S13, the fluctuation of the average power of

illumination is within ± 1 dB. In our work, we found that the photoresponsivity of the nanowire decays about 100 times from 0 to 10000Hz. The fluctuation of light illumination intensity can be neglected.

References

1. Anderson, B.; Anderson, R., *Fundamentals of Semiconductor Devices*. McGraw-Hill, Inc., 2004.
2. Landauer, R.; Swanson, J., Diffusion Currents in the Semiconductor Hall Effect. *Phys. Rev.* **1953**, *91*, 555-560.
3. Seiffe, J.; Hofmann, M.; Rentsch, J.; Preu, R., Charge Carrier Trapping at Passivated Silicon Surfaces. *J. Appl. Phys.* **2011**, *109*, 064505.
4. Müller, W.; Mönch, W., Determination of Surface States at Clean, Cleaved Silicon Surfaces from Photoconductivity. *Phys. Rev. Lett.* **1971**, *27*, 250-253.
5. Tan, S. L.; Zhao, X.; Chen, K.; Crozier, K. B.; Dan, Y. P., High-Performance Silicon Nanowire Bipolar Phototransistors. *Appl. Phys. Lett.* **2016**, *109*, 033505.